論文の内容の要旨

論文題目　**Development Study on Mass Transport Measurement Systems and Crystallization Reactor Systems in Microfluidic Devices for Integrated Chemical Processes**
（集積化学プロセスのためのマイクロ流体デバイス内における物質輸送計測システム
および結晶合成システムの開発に関する研究）

氏　名　　篠原　恭介

1. Introduction

A number of microfluidic devices have been developed recently for chemical analysis applications in the form of μ-TAS (Micro-Total Analysis Systems) and labs-on-a-chip [1]. Microfluidic device is fluid machinery, which consists of several microchannels. These μ-TAS and labs-on-a-chip have many advantages such as increased speed, efficiency, portability, and reduced consumption. In order to utilize these advantages, chemical processes such as mixing, reaction, and solvent extraction were integrated onto a microchip using a multiphase microflow network [2]. The investigation of the fluid mechanics and mass transport is therefore very important for effective design of microfluidic devices.

In this thesis, I have developed the *in situ* mass transport measurement systems including a micro-LIF system, a high-speed micro-PIV system, and a 3D scanning micro-PIV system. Furthermore, utilizing the findings, I have applied microfluidic devices in order to explore material science and crystal engineering: A Fullerene C_{60} crystallization reactor system was developed by utilizing such a microfluidic liquid/liquid interface.

2. Development of Mass Transport Measurement System: 3D scanning micro-PIV

To obtain three-dimensional velocity distribution in microscopic scale, a novel particle image velocimetry system was developed (Figure 1a). To validate the measurement accuracy of the system, the developed 3D scanning micro-PIV technique was applied to a microtube flow measurement (Figure 1b). The flow in a micro-round tube with 95 μm diameter was visualized using fluorescent particles, which absorbed green light (~535 nm) and emitted orange light (~575 nm). In the 3D scanning micro-PIV technique, 2D (x,y)-2C (u,v) velocity was calculated using a cross correlation method, which is most popular for digital particle image velocimerty. In order to obtain information on the vertical axis (z), the objective lens was equipped with a piezo actuator. The piezo actuator was displaced by the input current signal from a function generator. The amplitude and frequency of displacement were determined by the voltage and frequency of the input current signal, respectively. Thus, when the piezo actuator was displaced in z direction, the objective lens also moved and one can obtain information on the vertical axis. In addition, Out-of-plane velocity (w) was calculated using a dual-plane PIV technique [3].

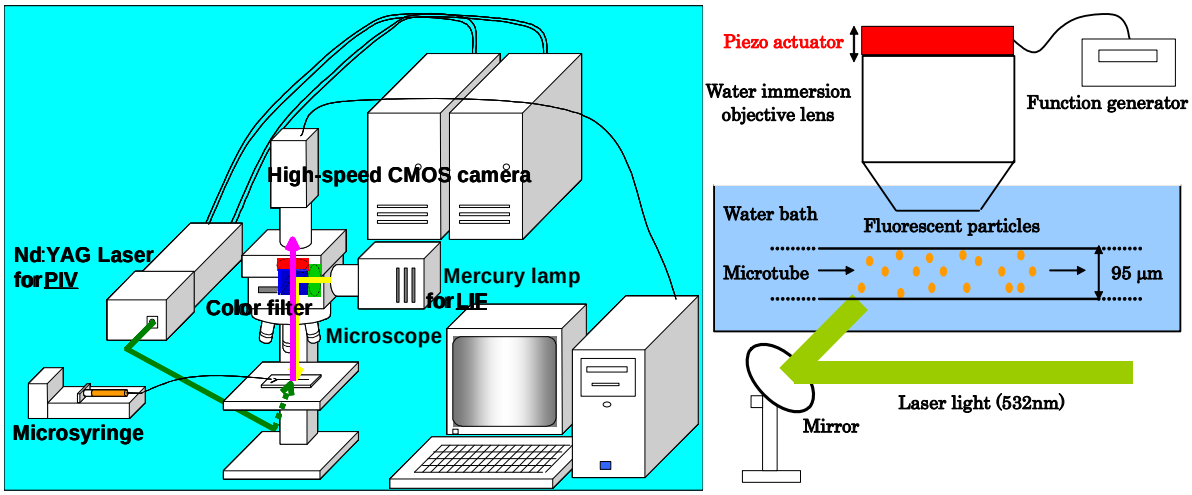

(a)　　(b)

Figure 1 (a) Schematic of experimental setup and (b) 3D scanning micro-PIV system

2.2 Microscopic 3Dimensional and 3 component flow velocity distribution

Figure 2a shows optical micrographs of the test section. The microtube was made of FEP (Fluorinated Ethylene Polymer). The refractive index 1.338 was almost similar to that of water (1.330). Since the mictotube was set in a

water bath shown in Figure 1b, the near wall regions were clearly observed inside the microtube flow. Figure 2b shows the three-dimensional velocity and three-component distribution of the microtube flow. The working fluid of water was injected at the constant flow rate of 4.0 μL/min, corresponding Reynolds number was 0.91. The velocity distribution was obtained at a spatial resolution of 5.4 x 2.7 x 4.2 μm. The microtube was set parallel to the *x*-axis and the test fluids flowed from back to front. While the velocity component was almost zero at the near wall region, the maximum velocity was observed at the center of the microtube. The velocity distribution had the appearance of typical, fully developed laminar flow. The obtained velocity profiles agreed with theoretical solution of Hagen-Poiseilles equation. On the measurement accuracy of the 3D scanning micro-PIV system, the maximum temporal variance was RMS = 1.6 mm/s in streamwise velocity component. In other hand, the depthwise velocity (*w*) of the microtube flow was negligible small. Thus, this was not suitable test section for the validation of the out of plane velocity.

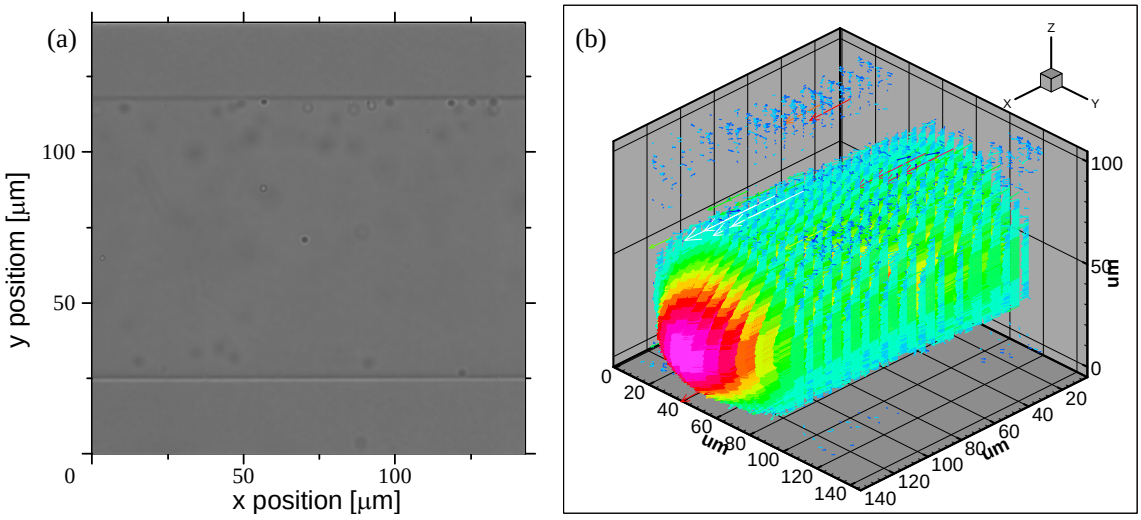

Figure 2 (a) Optical micrograph of the microtube and (b) 3D-3C velocity distribution.

3. Development of Crystallization Reactor System: A Microfluidic Synthesis of C_{60} Single Crystals

3.1 Screening of Fullerene C_{60} crystals

Since their initial discovery in 1985, Fullerenes C_{60} have attracted significant attention for their unique physical and chemical properties, and have resulted in the creation of a new research field. Fullerene C_{60} is also excellent candidate of new medicine. Since the metastable crystals showed different solubility and bioavailability from those of stable crystals, screening of metastable or stable phases of crystals is critical for development of new medicine. In terms of protein crystals, efficient screening techniques using microfluidic chips had already been presented. In this thesis, I have developed a screening method of C_{60} crystallization using a microfluidic device. The test solutions were toluene with C_{60} and alcohol, including isopropanol, ethanol, and methanol. In all the experiments, the concentration of C_{60} dissolved in toluene was a quarter of the saturation concentration at 25 ^{o}C. Two solutions were kept at a low temperature of 0 ^{o}C by a temperature controller until just before introduction into the channels. Toluene and alcohol were introduced into a Y-shaped glass microchannel with 100 μm width, 40 μm depth and 40 mm length independently with a flow rate of 1.0 μL/min (Fig. 3a). The C_{60} crystals precipitated at the toluene/alcohol interface [4]. The microchannel was immersed in a water bath and a water immersion objective lens (*M* = 100, *NA* = 1.0) was used for in situ observations (Fig. 3b). The room temperature was kept at 20 ^{o}C using an air conditioner. The starting water temperature was 5 ^{o}C as set by the temperature controller until just before introduction of the test solutions. Subsequently, the water bath was left out at room temperature. Therefore, the temperature of the water bath increased and approached 20 ^{o}C gradually during the experiments. The water bath temperature was constantly checked by a thermometer.

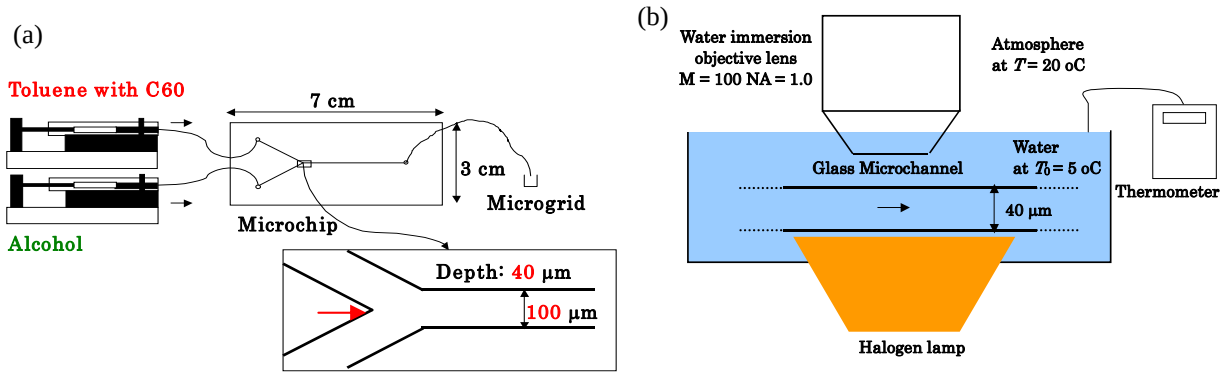

Figure 3(a) Schematic of microchannel and (b) temperature control system

3.2 Structural and optoelectonic properties of C_{60} crystals

In the first experiment, I introduced toluene with C_{60} and IPA into the channels. Within 5 minutes after the fluid flow was stopped, at the bath temperature of 6 ^{o}C, C_{60} crystals were formed in Fig. 4a-b. The lengths of the crystals were approximately 30 μm. The center axis areas of the crystals were semi-transparent in left inset Fig. 4a-b. In addition, several crystals had crosswise cut edges in right inset Fig. 4a-b. SEM (Scanning Electron Microscopy) revealed the reason for the formation of the semi-transparent whiskers in Fig. 4b-a. Several "macaroni"-like crystals with 7 μm diameter were observed. Their cross-sections were hexagonal. Another type of tube which was cut crosswise at the edge was also observed in Fig. 4b-b. The edge outline was not parallel to the center axis, indicating that the cross-sections of these "penne"-like crystals were also hexagonal. The characteristics of the cross-sections of these crystals were emphasized in another magnified SEM image in Fig. 4b-c. Within the void area, multi-layers of the crystal were observed. The cross-section of the void was not circular but was hexagonal. Some spherical crystals shown in Fig. 4b-d were also observed on the same microgrid. Within 15 minutes after the flow was stopped, at a bath temperature of 9 ^{o}C, tree-like dendrites appeared in Fig. 4a-c. A number of branches were observed to sprout from a main trunk. The main trunks and the branches were approximately 50 μm and 10 μm in length, respectively. The main trunks originated at the upper channel wall, indicating that nucleation of the crystals occurred at the wall on the toluene side. Thirty-two minutes after the flow was stopped, at a bath temperature of 16 ^{o}C, short rhombus-shaped columns with 10 μm length were formed in Fig. 4b-e. Forty minutes after the flow was stopped, at a bath temperature of 18 ^{o}C, the typical C_{60} nanowhiskers with high aspect ratios appeared in Fig. 4b-f. Their lengths and diameters were more than 20 μm and less than 5 μm, respectively.

To change the solvated state and the supersaturation of C_{60} from the conditions of the previous studies, in the second experiment, we attempted to use ethanol instead of IPA. One minute after the flow was stopped, at a bath temperature of 5 ^{o}C, crystals with hollow ends appeared on the toluene side in Fig. 4a-d. The size was about 4 μm in diameter and 30 μm in length. A TEM (Transmission Electron Microscope) micrograph showed the outline of the open side void in Fig. 4c-a. Five minutes after the flow was stopped, at a bath temperature of 7 ^{o}C, many particles of a few micrometers size were formed on the toluene side in Fig. 4a-e. Several sprouts from the particles were also observed (right arrow in Fig. 4a-e). The sprouts grew in one direction. On the other hand, a Y-shaped branch crystal was also observed (left arrow). The Y-shaped crystal had two (Fig. 4c-b) or three (Fig. 4c-c) of the small separation branches. Seven minutes after the flow was stopped, at a bath temperature of 8 °C, several crystals with sharp edges appeared in Fig. 4a-f. The crystals radiated in all directions and became multiple pods. The crystals had 6-8 columns with two- (Fig. 4c-d) or three-dimensional structures (Fig. 4c-e). Some crystals had acute edges in Fig. 4c-f. The size of each crystal was about 20 μm, and interestingly, each other column was positioned at a regular angle of 60^{o}.

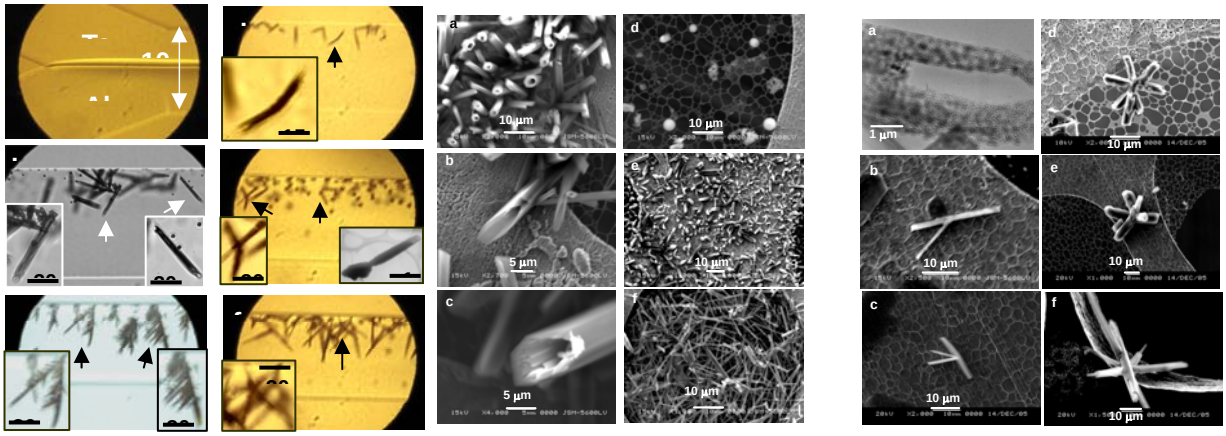

(a) (b) (c)

Figure 4 (a) Optical micrographs and SEM images of C_{60} crystals synthesized in (b) toluene-IPA and (c) toluene-ethanol systems

SAED (Selected Area Electron Diffraction) revealed that the C_{60} crystals synthesized in the microfluidic device had a hexagonal close-packed structure (hcp) or a face centered cubic (fcc) structure in Fig. 5a. The lattice constants were a = 19.2 Å and c = 9.7 Å (Fig. 5a-a) and a = 23.3 Å (Fig. 5a-b). They were found to be single crystallines. Overall, the lattice constants of these crystals were larger than those of pristine C_{60}: a = 14.2 Å. This indicated that the C_{60} crystals synthesized in the microfluidic device may be van der Waals crystals including the toluene molecules in the structure. All the Raman spectrum of the C_{60} crystals synthesized under different flow rate conditions during nucleation showed 8 H_g and 2 A_g modes, which corresponds to characteristic active modes of C_{60} single crystals (Fig.5b). Especially, $A_g(2)$ pentagonal pinch mode 1468 cm^{-1} showed the C_{60} crystals consisted of Fullerene monomers, indicating that any polymerization of C_{60} crystal did not occur in the microfluidic device during crystallization. In other hand, PL (Photoluminescence) spectra of the C_{60} crystals were unique (Fig.5c). The PL intensity of the rod-shaped crystal was 1 order of magnitude higher than that of bulk crystals (Fig.5c-a), suggesting that the doping by toluene molecules enhanced the luminescence of C_{60}. The difference of PL intensity was resulted from different lattice structure and proportion of included toluene molecules. In addition, it was obvious that 0.05 eV blueshift of PL spectra of the C_{60} rods was observed compared with those of the raw C_{60} materials (Fig. 5c-b). This indicated that distortion of fcc structure and the strong influence of toluene molecules on electronic state of the C_{60} rods.

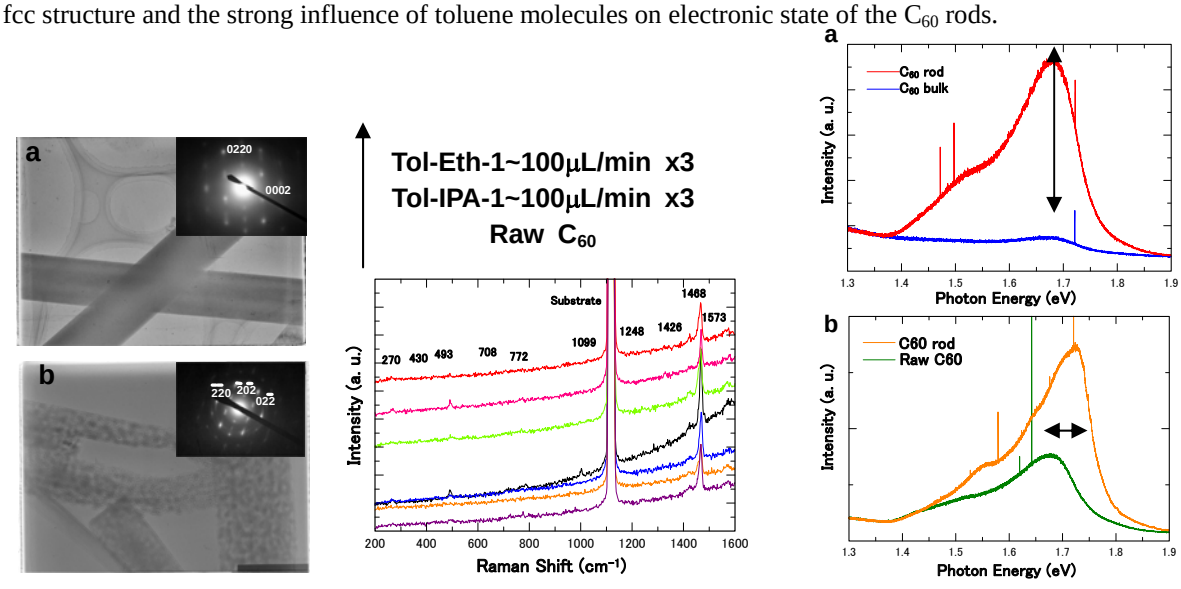

(a) (b) (c)

Figure 5 (a) SAED, (b) micro-Raman and (c) micro-photoluminescence spectra of C_{60} crystals

4. Conclusions

In order to investigate *in situ* microscopic scale fluid mechanics and mass transport, a micro-LIF system, a high-speed micro PIV system, and a 3D scanning micro-PIV system were developed. By using the systems, concentration and velocity fields inside the microfluidic devices were measured at previously unachieved high spatiotemporal resolutions and dimensions. In addition, by utilizing the insights obtained above, the Fullerene C_{60} crystallization

reactor was developed. The screening of metastable phases of C_{60} crystals were carried out and their structural and optoelectronic properties were investigated. The C_{60} crystals showed unique physical properties resulted from specific microfluidic environment. The present works provide physicochemical properties of microscopic fluid mechanics, mass transport, and crystallization. These insights will advance research fields of μ-TAS, lab-on-a chip, material science and crystal engineering.

References

[1] PS. Dittrich, K. Tachikawa, A. Manz, ***Anal. Chem.*** **78** 3887-3907 (2006).
[2] M. Tokeshi, T. Minagawa, K. Uchiyama, A. Hibara, K. Sato, H. Hisamoto, T. Kitamori, ***Anal. Chem.*** **74** 1565-1571 (2002).
[3] M. Raffel, M. Gharib, O. Ronneberger, J. Kompenhans, ***Exp. Fluids*** **19** 69-77 (1995).
[4] SH. Lee, K. Miyazawa, R. Maeda, ***Carbon*** **43** 887-889 (2005).